Analytical model for the thermal conductivity of fully ionized plasmas

Yuanjie Huang

Mianyang, *Sichuan province*, *People's Republic of China*

*Corresponding author's E-mail: hyj201207@163.com

Abstract

The thermal conductivity is a fundamental property of plasmas, yet its experimentally observed reduction remains an enigmatic phenomenon. Over the past half-century, extensive efforts have been dedicated to elucidating the mechanisms behind this reduced thermal conductivity and the associated heat-flux limiter, but a definitive solution has remained elusive. In this work, we present an analytical model for plasma thermal conductivity that is free of artificial parameters. This model employs Maxwell distributions for both electrons and ions and provides analytical expressions for thermal conductivity and the heat-flux limiter. Importantly, the predictions of the model are in good agreement with experimental observations. Its validity extends across plasmas with both small and large temperature gradients, significantly enhancing its applicability. This straightforward model not only offers insights into the underlying physics of reduced thermal conductivity and the heat-flux limiter but also plays a crucial role in advancing our understanding of thermal transport in plasmas across diverse areas.

keywords: plasma thermal conductivity, heat-flux limiter, analytical model,

The thermal conductivity is a fundamental property of plasmas that impacts a broad spectrum of scientific and technological domains, including nuclear fusion [1] and astrophysics [2]. Since the 1940s, extensive research has focused on the thermal conductivity of the ionized plasmas [3], with the seminal work of Spitzer and Härm (SH) [4] providing a cornerstone for classical understanding. However, experimental measurements have consistently revealed that the observed electron thermal conductivity is significantly lower than the values predicted by the classical SH theory [5, 6, 7].

To address this discrepancy, numerous theoretical efforts have been proposed, such as nonlocal heat transport arising from the delocalization of heat flux [8-11] and non-Maxwell-Boltzmann (n-MB) electron velocity distributions distorted by inverse bremsstrahlung (IB) absorption of laser light [12-16]. These theories often rely on arbitrary tuning parameters and remain challenging to verify quantitatively [2], despite experimental investigations into nonlocal electron heat transport [17] and n-MB electron distribution functions [18, 19, 20]. In simulation codes, an empirical heat-flux limiter has traditionally been employed to match the experimental temperature evolution of laser-heated plasmas [1, 7,11, 21, 22]. However, experimental measurements of the temporal and spatial evolution of electron density have shown that flux-limited heat transport is inconsistent with the spatial extent of plasma X-ray emission [17]. Overall, the observed reduction in electron thermal conductivity has been a subject of intense scrutiny for decades. Yet, the underlying physical mechanisms remain debated and elusive, making it a long-standing open question in plasma physics [1, 2].

In this work, we introduce a simple analytical model for the reduced thermal conductivity of plasmas and the phenomenological heat-flux limiter commonly used in simulations. This model employs Maxwell distribution functions for both electrons and ions, offering a straightforward approach to understanding these phenomena

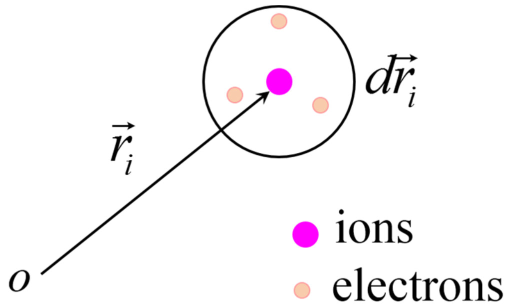

Figure 1 Schematic diagram for the local plasma in the mathematical micro-region with electrons (orange circles) and the ions (magenta circles).

To examine the physical properties of local plasmas in a steady state, charge neutrality is typically assumed due to the extremely short electric relaxation time, $\tau=\varepsilon_0\varepsilon/\sigma_e$. Here, τ represents the electron relaxation time required to reach electric equilibrium, σ_e denotes the electrical conductivity attributed to electrons, and ε_0 and ε correspond to the vacuum permittivity and the relevant dielectric constant, respectively. Under charge neutrality, the kinetic momentum of the local plasma is primarily determined by the ions. This is because ion masses are significantly greater than electron masses, causing the lighter electrons to move in concert with the heavier ions. Consequently, the position of a charge-neutral plasma in a mathematical micro-region with uniform number density and temperature can be represented by the ion position rather than the electron position. In such a micro-region, the electron and ion positions are indistinguishable, as illustrated in Fig. 1. Thus, the Maxwell distribution functions for ions and electrons can be expressed as

$$f_i^0 = \frac{n_i(\vec{r}_i, t)}{\pi^{3/2} v_{iT}^3(\vec{r}_i)} \exp\left[-\frac{v_i^2}{v_{iT}^2(\vec{r}_i)}\right] \tag{1}$$

$$f_e^0 = \frac{n_e(\vec{r}_i, t)}{\pi^{3/2} v_{eT}^3(\vec{r}_i)} \exp\left[-\frac{\vec{v}_{ei}^2}{v_{eT}^2(\vec{r}_i)}\right] \tag{2}$$

where f_i^0, f_e^0 denote the Maxwell distribution functions for the ions and electrons, respectively. $n_i(r_i, t)$, $n_e(r_i, t)$ represent the ion and electron number densities, which depend on the ion position r_i and time t. $v_{iT}(r_i)$ and $v_{eT}(r_i)$ are the position-dependent thermal velocities of the ions and electrons, respectively, and they satisfy the following relations [23].

$$v_{iT}(\vec{r}_i) = \sqrt{\frac{2k_B T_i(\vec{r}_i)}{m_i}}$$

$$v_{eT}(\vec{r}_i) = \sqrt{\frac{2k_B T_e(\vec{r}_i)}{m_e}}$$

where k_B represents the Boltzmann constant, m_i and m_e denote the ion and electron masses, respectively, while $T_i(r_i)$ and $T_e(r_i)$ describe the position-dependent ion and electron temperatures.

The most notable departure from the conventional SH theory lies in the electron Maxwell distribution function, where the position of electrons in the local plasma is determined by the ion position. This distinction is crucial for the subsequent theoretical development.

Based on the SH theory [4, 23], the distribution functions for ions and electrons during the transport process can be expressed as the sum of an isotropic term and an anisotropic term, as shown below:

$$f_i = f_i^0 + f_i^1$$

$$f_e = f_e^0 + f_e^1$$

where f_e^0 and f_e^1 denote the isotropic and anisotropic components of the electron distribution function, respectively. Similarly, f_i^0 and f_i^1 represent the isotropic and anisotropic components of the ion distribution function.

Based on the non-equilibrium Boltzmann transport equation and the SH theory for electron thermal conductivity [3, 23, 24], the anisotropic component of the electron distribution function can be expressed as

$$\vec{v}_e \cdot \nabla_{\vec{r}_e} f_e^0 + \frac{e\vec{E}}{m_e} \cdot \nabla_{\vec{v}_e} f_e^0 = -\frac{f_e^1}{\tau_{ei}} \tag{3}$$

where r_e denotes the electron position, v_e is the electron velocity, e represents the electron charge, E is the electric field, and τ_{ei} is the electron relaxation time due to electron-ion collisions.

Because the electron position coincides with the ion position in the local plasma micro-region, the spatial gradient of the electron distribution function with respect to the electron position is zero.

$$\nabla_{\vec{r}_e} f_e^0 = 0 \tag{4}$$

This is a key step in the analysis. Substituting the electron Maxwell distribution function into Eq. (3) yields

$$f_e^1 = \tau_{ei} \frac{e\vec{E} \cdot \vec{v}_{ei}}{k_B T_e(\vec{r}_i)} f_e^0 \tag{5}$$

The electron current density can be expressed as

$$j_e = e\int d\vec{v}_{ei} \vec{v}_e f_e^1$$

Substituting Eq. (5) yields

$$j_e = \frac{8en_e \tau_{ei}}{\pi^{1/2} m_e} e\vec{E} \tag{6}$$

Similarly, the anisotropic component of the ion distribution function is given by

$$f_i^1 = -\tau_i f_i^0 \vec{v}_i \cdot \left[\nabla_{\vec{r}_i} \ln n_i(\vec{r}_i, \vec{v}_i, t) + \frac{\vec{v}_i^2}{v_{iT}^2(\vec{r}_i)} \nabla_{\vec{r}_i} \ln T_i(\vec{r}_i) - \frac{3}{2} \nabla_{\vec{r}_i} \ln T_i(\vec{r}_i) + \frac{Ze\vec{E}}{k_B T_i(\vec{r}_i)} \right] \tag{7}$$

where τ_i denotes the ion relaxation time due to the ion-ion collisions. Therefore, the electrical current density induced by the directional drift of ions can be expressed as

$$j_i = -Ze\int d\vec{v}_i \vec{v}_i f_i^1$$

where Z denotes the net charge of the ion. Combining Eq. (7) with the above expression yields the ion current density in Eq. (8).

$$j_i = \frac{8Zen_i \tau_i k_B T_i(\vec{r}_i)}{\pi^{1/2} m_i} \cdot \left[\nabla_{\vec{r}_i} \ln n_i(\vec{r}_i, \vec{v}_i, t) + \frac{5}{2} \nabla_{\vec{r}_i} \ln T_i(\vec{r}_i) + \frac{Ze\vec{E}}{k_B T_i(\vec{r}_i)} \right] \tag{8}$$

During thermal transport, the electrical transport processes are typically much faster than thermal transport, leading to the charge neutrality assumption that the total electrical current is zero. This assumption, widely used in related theoretical studies [4, 9, 12, 23, 24, 25], allows one to derive the electric field using Eq. (6) and (8):

$$e\vec{E} = -\frac{\frac{\tau_i}{m_i} k_B T_i(\vec{r}_i)}{\left(\frac{\tau_{ei}}{m_e} + \frac{Z\tau_i}{m_i}\right)} \left[\nabla_{\vec{r}_i} \ln n_i(\vec{r}_i, \vec{v}_i, t) + \frac{5}{2} \nabla_{\vec{r}_i} \ln T_i(\vec{r}_i) \right] \tag{9}$$

The electron thermal current density is given by [23, 24]

$$q_e = \int d\vec{v}_{ei} \frac{1}{2} m_e v_{ei}^2 \vec{v}_e f_e^1$$

where q_e denotes the electron thermal current density. Using Eq. (5), the electron thermal current density can be calculated as

$$q_e = \frac{32 n_e \tau_{ei} k_B T_e(\vec{r}_i)}{\pi^{1/2} m_e} e\vec{E}$$

Given that electron mobility is much larger than ion mobility ($\tau_{ei}/m_e >> Z\tau_i/m_i$) [23], substituting Eq. (9) into the electron thermal current density yields

$$q_e \approx -\frac{32 n_e k_B^2 T_e(\vec{r}_i) T_i(\vec{r}_i)}{\pi^{1/2}} \frac{\tau_i}{m_i} \left[\frac{5}{2} \frac{1}{L_T} + \frac{1}{L_n} \right] \tag{10}$$

where L_T and L_n represent the temperature-gradient scale length and the number density-gradient scale length, respectively. These quantities are commonly defined in the literatures [12, 23-26]

$$\frac{1}{L_n} = \nabla \ln n_i(\vec{r}_i, t)$$

$$\frac{1}{L_T} = \nabla \ln T_i(\vec{r}_i, t)$$

Hence, the electron thermal conductivity can be expressed as

$$\kappa_e = \frac{32 n_e k_B^2 T_e(\vec{r}_i)}{\pi^{1/2}} \frac{\tau_i}{m_i} \left[\frac{5}{2} + \frac{L_T}{L_n} \right] \tag{11}$$

where κ_e denotes the electron thermal conductivity. This formulation indicates that the electron thermal conductivity depends on the ion mobility (τ_i/m_i) rather than the electron mobility (τ_{ei}/m_e), a key departure from the classical SH theory. This property likely arises from charge neutrality, which requires electrons and ions to move collectively in the local plasma micro-region.

Similarly, the ion thermal current density is given by

$$q_i \approx -\frac{32n_i\left[k_B T_i(\vec{r}_i)\right]^2}{\pi^{1/2}}\frac{\tau_i}{m_i}\left[\frac{7}{2}\frac{1}{L_T}+\frac{1}{L_n}\right] \tag{12}$$

where q_i signifies the ion thermal current density. The ion thermal conductivity can be expressed as

$$\kappa_i = \frac{32n_i k_B^2 T_i(\vec{r}_i)}{\pi^{1/2}}\frac{\tau_i}{m_i}\left[\frac{7}{2}+\frac{L_T}{L_n}\right] \tag{13}$$

where κ_i denotes the ion thermal conductivity.

The total heat flux, q_t, is obtained by summing the electron and ion thermal current densities:

$$q_t = -\frac{32k_B T_i(\vec{r}_i)}{\pi^{1/2}}\frac{\tau_i}{m_i}\left[n_e k_B T_e(\vec{r}_i)\left(\frac{5}{2}\frac{1}{L_T}+\frac{1}{L_n}\right)+n_i k_B T_i(\vec{r}_i)\left(\frac{7}{2}\frac{1}{L_T}+\frac{1}{L_n}\right)\right] \tag{14}$$

The combined plasma thermal conductivity, contributed by both electrons and ions, is given by

$$\kappa_t = \frac{32k_B}{\pi^{1/2}}\frac{\tau_i}{m_i}\left[n_e k_B T_e(\vec{r}_i)\left(\frac{5}{2}+\frac{L_T}{L_n}\right)+n_i k_B T_i(\vec{r}_i)\left(\frac{7}{2}+\frac{L_T}{L_n}\right)\right] \tag{15}$$

In laser-plasma experiments, the temperature gradient is often much larger than the density gradient in the transport domain between the laser ablation surface and the laser absorption critical surface ($L_T \ll L_n$) [5, 23]. Consequently, the plasma thermal conductivity and heat flux can be simplified as

$$\kappa_t = \frac{32 n_e k_B^2 T_e(\vec{r}_i)}{\pi^{1/2}} \frac{\tau_i}{m_i} \left[\frac{5}{2} + \frac{7}{2Z} \frac{T_i(\vec{r}_i)}{T_e(\vec{r}_i)} \right]$$

$$q_t \approx -\frac{32 k_B T_i(\vec{r}_i)}{\pi^{1/2}} \frac{\tau_i}{m_i} \left[\frac{5}{2} n_e k_B T_e(\vec{r}_i) + \frac{7}{2} n_i k_B T_i(\vec{r}_i) \right] \frac{1}{L_T}$$

For comparison, the conventional SH thermal conductivity and the free-streaming limit for heat flux are given by [5, 23, 27, 28]

$$\kappa_{SH} = \frac{32 n_e k_B^2 T_e}{\pi^{1/2}} \frac{\tau_{ei}}{m_e}$$

$$q_f = n_e k_B T_e(\vec{r}_i) \left[\frac{k_B T_e(\vec{r}_i)}{m_e} \right]^{1/2}$$

where κ_{SH} denotes the classical SH thermal conductivity, and q_f signifies the free-streaming limit.

The thermal conductivity ratio κ_t/κ_{SH} and the heat-flux limiter f can be derived based on the relaxation time expressions [23],

$$\frac{\kappa_t}{\kappa_{SH}} = \frac{\sqrt{2}}{Z^2} \sqrt{\frac{m_e}{m_i}} \left[\frac{T_i(\vec{r}_i)}{T_e(\vec{r}_i)} \right]^{3/2} \left[\frac{5}{2} + \frac{7}{2} \frac{T_i(\vec{r}_i)}{T_e(\vec{r}_i)} \right] \tag{16}$$

$$f = -\frac{32}{\pi^{1/2} Z^2} \sqrt{\frac{m_e}{m_i}} \frac{\lambda_e}{L_T} \left[\frac{T_i(\vec{r}_i)}{T_e(\vec{r}_i)} \right]^{5/2} \left[\frac{5}{2} + \frac{7}{2} \frac{T_i(\vec{r}_i)}{T_e(\vec{r}_i)} \right] \tag{17}$$

where λ_e denotes the electron mean free path. The ratio κ_t/κ_{SH} is proportional to the square root of the electron-to-ion mass ratio and varies as $(T_i/T_e)^{3/2}$ approximately.

To validate this theory, comparisons between experimental estimates and theoretical predictions for κ_t/κ_{SH} and f are essential. In laser-plasma experiments, physical variables such as electron temperature, ion temperature, and the ratio λ_e/L_T vary with position and time [29]. Consequently, κ_t/κ_{SH} and f must also vary spatially and temporally, consistent with simulations of direct-drive target implosions [30].

Thus, constant values for these parameters may not fit experimental results accurately.

For example, in long-pulse laser experiments with $T_e \approx T_i$ and $\lambda_e/L_T \approx 0.04$ for hydrogen plasma [6, 7], Eq. (17) yields a heat-flux limiter value of $f\approx 0.1$, which aligns with simulation results of $0.06<f<0.1$ [6]. Under these conditions, Eq. (16) gives $\kappa_t/\kappa_{SH} \approx 0.2$, consistent with experimental estimates of 0.4 ± 0.2 [6].

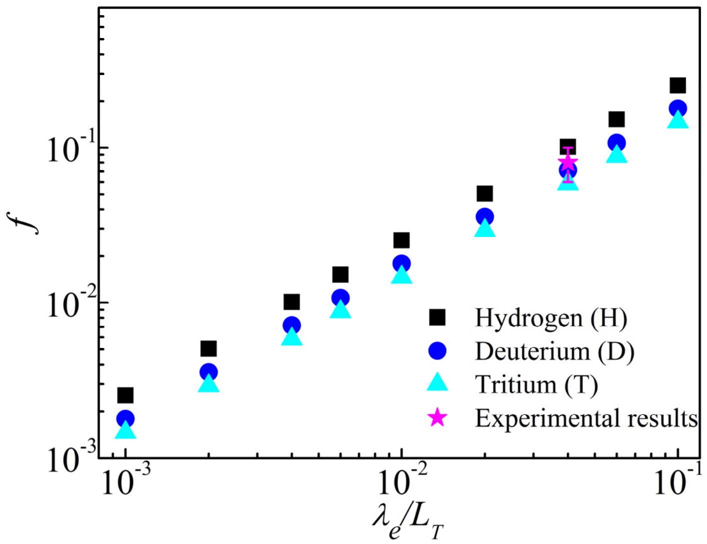

Figure 2. Comparison between the experimental heat-flux limiter [6](magenta pentagram with the error bar) and the predicted heat-flux limiters versus the ratio of the electron mean free path to the temperature-gradient scale length for the fully ionized hydrogen (black squares), deuterium (blue circles) and tritium (cyan triangles) plasmas, based on Eq. (17). The electron temperature is assumed to be the same as the ion temperature in the plasmas.

In short-pulse laser experiments with hydrogen plasma, where the peak electron temperature is $T_e \approx 5T_i$ and $\lambda_e/L_T = 0.5$ [7], the heat-flux limiter f calculated using Eq. (15) and the free-streaming limit definition [7] is $f\approx 0.02$. As time progresses and λ_e/L_T

decreases, T_e approaches the nearly constant T_i [29], and the heat-flux limiter increases to $f \approx 0.06$. Thus, the calculated range for f is $0.02<f<0.06$, which matches experimental observations of 2%–5% [7].

The consistency between theoretical results and experimental estimates suggests the validity of the proposed model.

Lastly, the validity of the model should be discussed. The theoretical treatments described above require the conditions $f_e^1/f_e^0 \ll 1$ and $f_i^1/f_i^0 \ll 1$. Based on Eqs. (5), (7), and (9), the ratios can be expressed as follows:

$$\frac{f_e^1}{f_e^0} \approx -\frac{5\sqrt{2}}{2Z^2}\sqrt{\frac{m_e}{m_i}}\frac{T_i(\vec{r}_i)}{T_e(\vec{r}_i)}\frac{\lambda_e}{L_T}$$

$$\frac{f_i^1}{f_i^0} \approx -\frac{5\sqrt{2}}{2Z^2}\frac{\lambda_e}{L_T}\left[\frac{T_i(\vec{r}_i)}{T_e(\vec{r}_i)}\right]^2$$

For experiments with a small temperature gradient ($\lambda_e/L_T \ll 1$), these conditions are easily satisfied. In high-power experiments with a large temperature gradient ($\lambda_e/L_T \sim 1$) and significantly higher electron temperatures than ion temperatures ($T_i(r_i) \ll T_e(r_i)$) [7, 29], the required conditions can still be met. In other words, the model appears to be valid for both small and large temperature gradients in relevant plasma experiments. Additionally, the relaxation times for electrons and ions are of critical importance. These relaxation times are widely believed to be dominated by small-angle scatterings [23]. During these small-angle scatterings, the electron screening effect should be considered for the ion charge, as it will reduce the scattering rate and increase the relaxation time to some extent.

In summary, we have developed an analytical model for the reduced thermal conductivity in the plasmas, based on the classical SH theory and Maxwell distribution functions for electrons and ions. This model provides accurate estimates of plasma thermal conductivity and heat-flux limiters, validated against experimental results. Unlike the classical SH theory, which is limited to plasmas with small temperature gradients, the model is applicable to both small and large temperature gradients. This broader applicability enhances our understanding of plasma behavior across diverse conditions and has significant implications for plasma research in various scientific and technological contexts.

Reference

1. R. S. Craxton et al., *Phys. Plasmas* **22**, 110501 (2015).
2. T. D. Arber et al., *Front. Astron. Space Sci.* **10**, 1155124 (2023).
3. R. Landshoff, *Phys. Rev.* **76**, 904 (1949).
4. Lyman Spitzer Jr., Richard Härm, *Phys. Rev.* **89**, 977 (1953).
5. R. C. Malone et al., *Phys. Rev. Lett.* **34**, 721 (1975).
6. M. S. White et al., *Phys. Rev. Lett.* **35**, 524 (1975).
7. D. R. Gray et al., *Phys. Rev. Lett.* **39**, 1270 (1977).
8. J. F. Luciani et al., *Phys. Rev. Lett.* **51**, 1664 (1983).
9. J. R. Albritton et al., *Phys. Rev. Lett.* **57**, 1887 (1986).
10. G. P. Schurtz et al., *Phys. Plasmas* **7**, 4238 (2000).
11. E. M. Epperlein, R. W. Short, *Physics of Fluids B: Plasma Physics* **3**, 3092 (1991).
12. P. Mora, H. Yahi, *Phys. Rev. A* **26**, 2259 (1982).
13. J. P. Matte et al., *Plasma Phys. Control. Fusion* **30**, 1665 (1988).
14. E. M. Epperlein, R. W. Short, *Phys. Rev. E* **50**, 1697 (1994).
15. C. P. Ridgers et al., *Phys. Plasmas* **15**, 092311 (2008).
16. Nathaniel R. Shaffer et al., *Phys. Rev. E* **108**, 045205 (2023).
17. T. Ditmire et al., *Phys. Rev. Lett.* **80**, 720 (1998).
18. David Turnbull et al., *Nat. Phys.* **16**, 181 (2020).
19. A. L. Milder et al., *Phys. Rev. Lett.* **127**, 015001 (2021).
20. D. Turnbull et al., *Phys. Rev. Lett.* **130**, 145103 (2023).
21. M. Day et al., *Contrib. Plasma Phys.* **36**, 419 (1996).
22. N. G. Basov et al., *J. Soviet Laser Research* **10**, 438 (1989).
23. Shalom Eliezer, *The Interaction of High-Power Lasers with Plasmas* (Institute of Physics Publishing, London, UK, 2002), pp. 17-21, 183-198.
24. H. Takabe, *The Physics of Laser Plasmas and Applications—Volume 2* (Springer Series in Plasma Science and Technology, Cham, Switzerland, 2024), pp. 285-323.
25. D. Shvarts et al., *Phys. Rev. Lett.* **46**, 243 (1981).
26. A. R. Bell et al., *Phys. Rev. Lett.* **47**, 247 (1981).
27. Claire Ellen Max et al., *Phys. Rev. Lett.* **45**, 28 (1980).
28. M. G. Anuchin et al., *Sov. J. Quantum Electron* **19**, 207 (1989).
29. D. R. Gray, J. D. Kilkenny, *Plasma Physics* **22**, 81 (1980).
30. A. Sunahara et al., *Phys. Rev. Lett.* **91**, 095003 (2003).